Selection rules for second-harmonic generation in nanoparticles

M. Finazzi,[1,*] P. Biagioni,[1] M. Celebrano,[2] and L. Duò[1]
[1]*LNESS, Dipartimento di Fisica, Politecnico di Milano, Piazza Leonardo da Vinci 32, 20133 Milano, Italy*
[2]*ULTRAS-INFM-CNR, Dipartimento di Fisica, Politecnico di Milano, Piazza Leonardo da Vinci 32, 20133 Milano, Italy*
(Received 14 February 2007; revised manuscript received 23 May 2007; published 13 September 2007)

General selection rules for second-harmonic generation in isolated nanoparticles are derived from angular momentum and parity conservation laws. A set of rules is discussed as a function of the particle symmetry group and the polarization of the fundamental wavelength (FW) and second-harmonic fields. A few relevant cases of particle geometry and FW illumination are discussed as examples.

DOI: 10.1103/PhysRevB.76.125414 PACS number(s): 73.50.Fq, 73.63.Kv

I. INTRODUCTION

Second-harmonic generation (SHG) in optical media is a well-known nonlinear phenomenon involving three photons which was first demonstrated[1] in 1961 and whose peculiar behavior at boundaries was soon recognized.[2] Nevertheless, it was only in the early 1980s that nonlinear optical spectroscopy of surfaces and interfaces started to develop as a well-established analysis tool in a wide area of fields.[3] The interest in SHG lies in its ability to selectively probe surfaces and interfaces, since selection rules for SHG do not allow for dipole emission from the bulk of centrosymmetric materials, such as metals or elemental semiconductors. At the surface or interface, however, the symmetry of the bulk is broken and dipole generation is no longer forbidden. This peculiar property has determined the enormous spread of SHG-based techniques in the community of surface and interface physics.

In the last decade, a renewed attention has been dedicated to SHG following the development of nanotechnologies and the increasing interest in nano-optics.[4] Metal nanostructures, which can be very effective for field-enhancement and confinement processes at optical wavelengths, are widely studied both as suitable substrates for surface-enhanced spectroscopy techniques[5,6] or as possible targets for localized photothermal therapies.[7,8] To this aim, SHG provides the ideal tool to study the field distribution around metal nano-objects,[9] with the high sensitivity which is naturally provided by a nonlinear process.

When studying SHG from subwavelength objects, however, not only the symmetry of the bulk atomic structure of the optical material is to be taken into account but also the symmetry of the object itself. In fact, at variance with an ideally infinite interface, the overall shape of the nanoparticle plays a significant role in determining the conditions for efficient SHG. This was clearly recognized by Dadap *et al.*,[10] who theoretically addressed second-harmonic scattering from a sphere of centrosymmetric material excited by a plane wave, where the overall response vanishes in the electric dipole approximation owing to the presence of inversion symmetry, while the leading emission terms are a nonlocally excited electric dipole and a locally excited electric quadrupole. The analysis leads to a set of selection rules, which are valid for linearly and circularly polarized plane waves incident on a sphere of a centrosymmetric material.[11]

In the work by Dadap *et al.*, the nonlocally excited electric dipole is due to retardation effects along the propagation direction of the incident plane wave. Brudny and co-workers[12,13] have extended the analysis to illumination other than plane wave, showing how dipolar emission from spherical particles is possible also due to inhomogeneous transverse and/or longitudinal electromagnetic fields, for example, when the particle lies close to a surface.

Nowadays, microscopic techniques are sometimes employed to locally study field-enhancement processes, and, generally, high-numerical-aperture objectives or even scanning near-field optical microscopy is used.[4] In this case, the fundamental wavelength illumination is not a plane wave anymore, and strong field gradients, together with a nonvanishing longitudinal field component, can be present in the illumination area. Moreover, not only spherical particles but also more complex geometrical shapes are under extensive investigation for their promising behavior as resonators in nano-optics applications.[6] Although nanoscale SHG has already been discussed by Bozhevolnyi and Lozovski[9] for a few particle geometries excited by either far or near fundamental wavelength (FW) fields, a set of general validity selection rules for SHG might be helpful in addressing more complicated particle geometries and FW field distributions.

In this paper, selection rules for SHG in isolated nanoparticles are derived from parity and angular momentum conservation laws. The lowest-order nonzero term in the (electric and magnetic) multipole expansion of the FW and the second-harmonic (SH) fields is given for different particle symmetry groups and incident field polarizations. Some peculiar geometries are then addressed and discussed as examples for their importance.

II. CONSERVATION OF PARITY AND ANGULAR MOMENTUM

In a SHG process, two photons in the FW electromagnetic field are annihilated and their energy transferred to a photon in a field oscillating at double frequency. Using perturbation theory, the cross section σ of this three-photon process can be expressed by a third-order term of the form

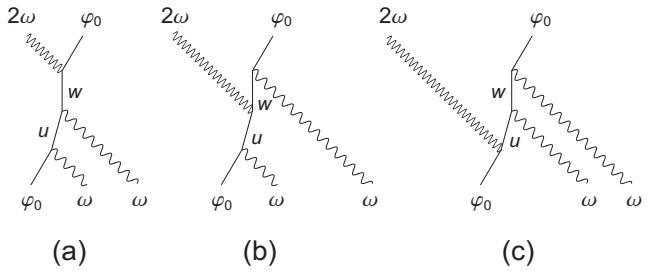

FIG. 1. The Feynman diagrams corresponding to second-harmonic generation.

$$\sigma \propto \left| \sum_{u,w} \frac{\langle \varphi_0|\hat{\mathbf{p}}\cdot\mathbf{A}_\omega|u\rangle\langle u|\hat{\mathbf{p}}\cdot\mathbf{A}_\omega|w\rangle\langle w|\hat{\mathbf{p}}\cdot\mathbf{A}_{2\omega}|\varphi_0\rangle}{[(E_u-E_0)-\omega+i\Gamma_u][(E_w-E_u)-\omega+i\Gamma_w]} + \frac{\langle \varphi_0|\hat{\mathbf{p}}\cdot\mathbf{A}_\omega|u\rangle\langle u|\hat{\mathbf{p}}\cdot\mathbf{A}_{2\omega}|w\rangle\langle w|\hat{\mathbf{p}}\cdot\mathbf{A}_\omega|\varphi_0\rangle}{[(E_u-E_0)-\omega+i\Gamma_u][(E_w-E_u)+2\omega]} + \frac{\langle \varphi_0|\hat{\mathbf{p}}\cdot\mathbf{A}_{2\omega}|u\rangle\langle u|\hat{\mathbf{p}}\cdot\mathbf{A}_\omega|w\rangle\langle w|\hat{\mathbf{p}}\cdot\mathbf{A}_\omega|\varphi_0\rangle}{[(E_u-E_0)+2\omega][(E_w-E_u)-\omega+i\Gamma_w]} \right|^2, \quad (1)$$

where φ_0 is the particle ground state, u and w are eigenfunctions corresponding to excited states of the unperturbed particle, and E_0, E_u, and E_w are the corresponding energies. The three terms in the sum correspond to the Feynman diagrams shown in Fig. 1. In this expression, $\hat{\mathbf{p}}$ is the particle momentum quantum operator, $\mathbf{A}_{2\omega}$ is the SH vector potential, and $\mathbf{A}_\omega$ is the vector potential of the *externally applied* FW field. The FW field generated by the particle should not be added to $\mathbf{A}_\omega$ in Eq. (1) since the interaction between the particle and the field the particle produces represents an internal self-interaction. The latter is accounted for by the particle eigenfunctions u and w, which describe excited electronic states as well as plasmon modes.

We consider the multipole expansions of the matrix elements describing the interaction of the particle with the SH and FW fields in Eq. (1). Let L'_ω and L''_ω be the L^2 quantum numbers of the two FW absorbed photons, M'_ω and M''_ω their L_z quantum numbers (z being an arbitrary quantization axis), and $L_{2\omega}$ and $M_{2\omega}$ the respective quantum numbers for the emitted SH photon. The Feynman diagram in Fig. 1(a) gives a contribution to Eq. (1) that can be expressed as the sum of terms T defined as follows:

$$T^{u,w}_{L'_\omega,M'_\omega,L''_\omega,M''_\omega,L_{2\omega},M_{2\omega}} \propto \langle \varphi_0|\hat{\mathbf{p}}\cdot\mathbf{A}(L'_\omega,M'_\omega)|u\rangle \times\langle u|\hat{\mathbf{p}}\cdot\mathbf{A}(L''_\omega,M''_\omega)|w\rangle \times\langle w|\hat{\mathbf{p}}\cdot\mathbf{A}(L_{2\omega},-M_{2\omega})|\varphi_0\rangle, \quad (2)$$

where $\hat{\mathbf{p}}\cdot\mathbf{A}(L,M)$ represents the electric (E) or magnetic (M) multipole operator of order (L,M). $M_{2\omega}$ is taken with a negative sign since the emitted SH photon carries the corresponding L_z angular momentum component *away* from the particle. Similar terms can be given for the other Feynman diagrams in Fig. 1.

The selection rules that determine the conditions for which a given T term is identically zero depend on how the multipoles in Eq. (2) transform under the particle symmetry group operations. For instance, the ground as well as the excited states of a particle with spherical symmetry are eigenstates of both L^2 and L_z. Therefore, the SH photon angular momentum must correspond to the sum of the angular momenta of the two FW incoming photons. On the other hand, in cylindrical symmetry, only the projection of the photon angular momentum along the symmetry axis (taken as the quantization axis z) needs to be conserved.

The photon parity conservation must be respected for particles exhibiting an inversion symmetry center, axis or plane. Considering inversion with respect to the origin, electric and magnetic multipoles of order (L,M) have opposite parity, corresponding to $(-1)^L$ and $(-1)^{L+1}$, respectively.[14] Electric multipoles of order (L,M) are symmetric (antisymmetric) with respect to reflection by a plane perpendicular to the quantization axis when $L+M$ is even (odd), while magnetic multipoles are symmetric (antisymmetric) when $L+M$ is odd (even).[14] Considering inversion with respect to the quantization axis, electric and magnetic multipoles of order (L,M) have the same parity, given by $(-1)^M$.[14]

TABLE I. SHG selection rules for the different particle symmetries illustrated in Fig. 2. Conservation of angular momentum for spherical symmetry corresponds to a condition involving a 3-j symbol (Ref. 15).

Symmetry and point group[a]	Selection rule
Spherical	$\begin{pmatrix} L'_\omega & L''_\omega & L_{2\omega} \\ M'_\omega & M''_\omega & -M_{2\omega} \end{pmatrix} \neq 0$ and $[(-1)^{L'_\omega+L''_\omega+L_{2\omega}+m}=1]$[b]
Cylindrical	$M'_\omega+M''_\omega-M_{2\omega}=0$
Central, S_2	$[(-1)^{L'_\omega+L''_\omega+L_{2\omega}+m}=1]$[b]
Axial, C_2	$(-1)^{M'_\omega+M''_\omega-M_{2\omega}}=1$
Reflection, C_{1h}	$[(-1)^{L'_\omega+M'_\omega+L''_\omega+M''_\omega+L_{2\omega}-M_{2\omega}+m}=1]$[b]

[a]Schoenflies notation, see Ref. 16.
[b]The value m indicates the number of *magnetic* multipole transitions involved in the T term.

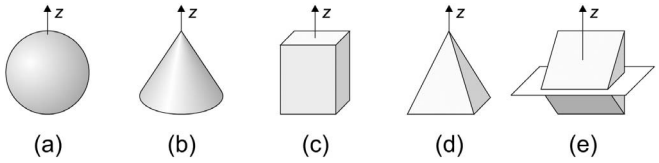

FIG. 2. The particle symmetry groups discussed in the text and referred to z quantization axis: (a) spherical, (b) cylindrical, (c) central, (d) axial, and (e) reflection symmetries across a mirror plane perpendicular to z, as shown.

By combining the symmetry properties of electric and magnetic multipoles with the conservation rules imposed by the particle symmetry groups, one can provide selection rules for the SHG process. Table I reports the conditions giving nonvanishing transition cross sections for a given combination of multipoles in the various particle symmetries illustrated in Fig. 2. If the particle symmetry is given by a combination of symmetry groups, the corresponding conditions listed in Table I must be satisfied at the same time. For instance, SHG from particles with C_{2h} symmetry must obey both the selection rules for axial (C_2) and reflection (C_{1h}) symmetries with respect to the same quantization axis. For the same reason, when the particle exhibits two (or three) orthogonal symmetry axes, the corresponding selection rules must be simultaneously satisfied by the field multipole expansions expressed by using either one of the symmetry axes as the quantization axis.

III. EMISSION PATTERNS AND LIGHT POLARIZATION

Let $\mathbf{k}_{2\omega}$ be the SH wave vector and $\mathbf{r}$ the distance from the particle. In the limit $k_{2\omega}r \gg 1$ (far field), the SH electric fields $\mathbf{E}^{(\mathrm{E})}_{L_{2\omega}M_{2\omega}}$ and $\mathbf{E}^{(\mathrm{M})}_{L_{2\omega}M_{2\omega}}$ produced by electric (E) or magnetic (M) multipoles of order $(L_{2\omega},M_{2\omega})$ are given by[14]

$$\mathbf{E}^{(\mathrm{E})}_{L_{2\omega},M_{2\omega}} = -(-i)^{(L_{2\omega}+1)}\frac{e^{ik_{2\omega}r}}{k_{2\omega}r}(\hat{\mathbf{u}}_r \times \mathbf{r} \times \nabla Y_{L_{2\omega}M_{2\omega}}), \quad (3a)$$

$$\mathbf{E}^{(\mathrm{M})}_{L_{2\omega},M_{2\omega}} = (-i)^{(L_{2\omega}+1)}\frac{e^{ik_{2\omega}r}}{k_{2\omega}r}\mathbf{r} \times \nabla Y_{L_{2\omega}M_{2\omega}}. \quad (3b)$$

Here, $\hat{\mathbf{u}}_r$ is a unit vector in the radial direction. $Y_{L_{2\omega}M_{2\omega}}$ is the spherical harmonic of order $(L_{2\omega},M_{2\omega})$.

Pure electric and magnetic multipoles of order $(L_{2\omega},M_{2\omega})$ have the same angular distribution of the time-averaged radiated power per solid angle $\frac{dP}{d\Omega}(L_{2\omega},M_{2\omega})$. A graphical representation of $\frac{dP}{d\Omega}(L_{2\omega},M_{2\omega})$ is given in Fig. 3 for dipoles $(L_{2\omega}=1)$ and quadrupoles $(L_{2\omega}=2)$.[14]

From Eqs. (3a) and (3b), one can also obtain the polarization state of the emitted SH light. Table II reports the direction of the electric far field for pure multipoles with $L_{2\omega} \leqslant 2$. The direction is indicated by a combination of the unit vectors $\hat{\mathbf{u}}_\theta$ and $\hat{\mathbf{u}}_\phi$ defined in a spherical coordinate system centered on the particle where θ and ϕ are the zenith and azimuth angles, respectively, the former being referred to the z quantization axis. An imaginary (real) ratio between the coefficients of $\hat{\mathbf{u}}_\theta$ and $\hat{\mathbf{u}}_\phi$ corresponds to a $\pi/2$ (zero) phase difference between the two field components and hence indicates elliptical (linear) polarization.

IV. DISCUSSION

Matrix elements of the form $\langle u|\hat{\mathbf{p}}\cdot\mathbf{A}(L,M)|w\rangle$ in the long-wavelength limit ($ka \ll 1$, a being the particle size and k the field wavelength) rapidly fall off with increasing multiple order L of the multipole $\hat{\mathbf{p}}\cdot\mathbf{A}(L,M)$.[14] The ratio $R(L)$ between matrix elements for successive orders, L and $(L+1)$, of either electric or magnetic multipoles of the same frequency is

$$R(L) \sim \frac{ka}{2L}. \quad (4)$$

The SHG cross section σ in Eq. (1) is given by the square of the sum of products involving three matrix elements, so only lowest-order contributions need to be taken into account. The analysis can be restricted to five distinct SHG mechanisms indicated, following the notation in Ref. 11, as E1+E1→E1, E1+E2→E1, E1+M1→E1, E1+E1→E2, and E1+E1→M1. In this notation, the first two symbols refer to the nature of the interaction with the FW field, and the third symbol describes the SH emission. The E1+E2→E1 interaction represents, for example, electric dipole (E1) emission that arises through combined electric dipole (E1) and electric quadrupole (E2) excitations. M1 indicates a magnetic dipole transition, which is of the same order in ka as an electric quadrupole transition.[11,14] If all five contributions are allowed, the SH field associated with the local E1+E1→E1 channel will be stronger than the other processes

TABLE II. SH electric field polarization for pure electric or magnetic multipoles with $L_{2\omega} \leqslant 2$. For each point in space, the unit vectors $\hat{\mathbf{u}}_\theta$ and $\hat{\mathbf{u}}_\phi$ are, respectively, parallel and perpendicular to the plane containing the z (quantization) axis, and are both perpendicular to the radial unit vector $\hat{\mathbf{u}}_r$.

	$M_{2\omega}=0$	$M_{2\omega}=\pm 1$	$M_{2\omega}=\pm 2$
$L_{2\omega}=1$ (E)	$\sin\theta\hat{\mathbf{u}}_\theta$	$e^{\pm i\phi}(\pm\cos(\theta)\hat{\mathbf{u}}_\theta + i\hat{\mathbf{u}}_\phi)$	
$L_{2\omega}=1$ (M)	$\sin\theta\hat{\mathbf{u}}_\phi$	$-e^{\pm i\phi}(i\hat{\mathbf{u}}_\theta \mp \cos(\theta)\hat{\mathbf{u}}_\phi)$	
$L_{2\omega}=2$ (E)	$-i\sin\theta\cos\theta\hat{\mathbf{u}}_\theta$	$e^{\pm i\phi}(\mp i\cos 2\theta\hat{\mathbf{u}}_\theta + \cos\theta\hat{\mathbf{u}}_\phi)$	$e^{\pm 2i\phi}\sin\theta(i\cos\theta\hat{\mathbf{u}}_\theta \pm \hat{\mathbf{u}}_\phi)$
$L_{2\omega}=2$ (M)	$-i\sin\theta\cos\theta\hat{\mathbf{u}}_\phi$	$-e^{\pm i\phi}(\cos\theta\hat{\mathbf{u}}_\theta \pm i\cos 2\theta\hat{\mathbf{u}}_\phi)$	$e^{\pm 2i\phi}\sin\theta(\pm\hat{\mathbf{u}}_\theta + i\cos\theta\hat{\mathbf{u}}_\phi)$

by a factor of the order of $(ka)^{-1}$, resulting in a $(ka)^{-2}$ higher radiating average power.

The E1+E1 $\rightarrow$E1 interaction violates parity conservation for *any* incident FW field distribution on S_2 symmetry particles since $(-1)^{L'_\omega+L''_\omega+L_{2\omega}}=(-1)^{1+1+1}=-1$. This channel is therefore forbidden for a centrosymmetric particle under more general conditions than those discussed in Refs. 10 and 11, which refer to plane-wave illumination. This transition may, however, be allowed for lower symmetry particles.

In general, in order to be able to apply the selection rules listed in Table I, one must know which are the relevant terms in the multipole expansion of the $\hat{\mathbf{p}}\cdot\mathbf{A}$ interaction Hamiltonian for a given FW field distribution on the particle. In the following, we will discuss a few important examples.

A. Plane-wave illumination

In an arbitrarily polarized FW plane wave propagating along the z direction, $\mathbf{A}=\mathbf{A}(0)e^{ikz}$, with $\mathbf{A}(0)\cdot\hat{\mathbf{u}}_z=0$. By expanding $\mathbf{A}$ around the particle position $z=0$, one finds (to first order)

$$\langle u|\hat{\mathbf{p}}\cdot\mathbf{A}|w\rangle \sim \frac{E_w-E_u}{\hbar\omega}\langle u|\mathbf{r}\cdot\mathbf{E}(0)|w\rangle + \langle u|\hat{\mathbf{L}}\cdot\mathbf{B}(0)|w\rangle + ik\langle u|\hat{p}_z[xA_x(0)+yA_y(0)]|w\rangle. \quad (5)$$

In this expression, $\mathbf{E}(0)$ and $\mathbf{B}(0)$ are the oscillating electric and magnetic fields at the particle position, $A_x(0)$ and $A_y(0)$ the (complex) components of $\mathbf{A}(0)$, and $\hat{\mathbf{L}}=\mathbf{r}\times\hat{\mathbf{p}}$. The three terms on the right-hand side of Eq. (5) correspond to E1, M1, and E2 transitions, respectively.

Let us first consider a circularly polarized plane wave, for which $A_y(0)=\pm iA_x(0)$, the plus or minus sign depending on the light helicity. In this case, thanks to the Wigner-Eckart theorem,[15] the E1 and M1 terms can be shown to be proportional to $\langle u|Y_{1\pm1,z}|w\rangle$, while the E2 term is proportional to $\langle u|Y_{2\pm1,z}|w\rangle$ (we have explicitly indicated the quantization axis which the spherical harmonics are referred to). These matrix elements correspond to transitions involving one FW photon with an L^2 quantum number $L_\omega=1$ (dipole transitions) or $L_\omega=2$ (quadrupole transitions) and an L_z quantum number $M_\omega=\pm1$. The sign of M_ω depends on the light helicity and is either positive or negative for all the terms in Eq. (5). The application of the selection rules in Table I is now straightforward. For instance, one can see that the E1+E1 $\rightarrow$E1 transition is forbidden under circularly polarized FW plane-wave illumination for spherical-symmetry particles, as $(-1)^{L'_\omega+L''_\omega+L_{2\omega}}=(-1)^{1+1+1}=-1$, and for cylindrical-symmetry particles, as $M'_\omega+M''_\omega-M'_{2\omega}=\pm1\pm1-M'_{2\omega}\neq0$. However, the transition becomes allowed for noncentrosymmetric particles that also violate cylindrical symmetry. In this case, SH emission is given by an E1 term with $M_{2\omega}=0$ ($M_{2\omega}=\pm1$) for C_2 (C_{1h}) symmetry, corresponding to SHG from an electric dipole oriented parallel (perpendicular) to z.

The lowest allowed SHG channel for S_2 particles displaying spherical or cylindrical symmetry around z and illuminated by a circularly polarized plane wave is E1+E1 $\rightarrow$E2.[10,11] The SH emission pattern can be only characterized by $M_{2\omega}=\pm2$ (see Fig. 3).[10,11] Other SH emission patterns become possible if the cylindrical symmetry is broken. A complete set of selection rules for different multipole transitions and particle symmetry groups under far-field circularly polarized plane-wave illumination is provided in Table IV (see the Appendix).

If we now turn to a linearly polarized FW plane wave with electric field pointing in the x direction, we have $\mathbf{A}_y(0)=0$. In this case, it is important to consider both the L_z and L_x photon quantum numbers. The choice of the quantization axis in turn determines the reference axis for the definition of the particle symmetry group. Let M_ω and $M_{2\omega}$ be the FW and SH photon L_z quantum numbers, and N_ω and $N_{2\omega}$ be the FW and SH photon L_x quantum numbers. When referred to the z quantization axis, the E1, M1, and E2 terms in Eq. (5) are proportional to $\langle u|Y_{11,z}+Y_{1-1,z}|w\rangle$, $\langle u|Y_{11,z}-Y_{1-1,z}|w\rangle$, and $\langle u|Y_{21,z}+Y_{2-1,z}|w\rangle$, respectively. Therefore, all these transitions involve FW photons with an M_ω quantum number that can be either +1 or −1 (but not 0). On the other hand, the E1, M1, and E2 terms are, respectively, proportional to $\langle u|Y_{10,x}|w\rangle$, $\langle u|Y_{11,x}+Y_{1-1,x}|w\rangle$, and $\langle u|Y_{21,x}+Y_{2-1,x}|w\rangle$ when referred to the x quantization axis, corresponding to photon L^2 and L_x quantum numbers equal to $(L=1,\ N=0)$, $(L=1,\ N=\pm1)$, $(L=2,\ N=\pm1)$, respectively. With this information, the rules in Table I can be applied considering either the z- or the x-quantization axis, thus obtaining the selection rules reported in the Appendix and listed in Tables V and VI, respectively. As for the particle symmetry groups, one must observe that particles with z-axis cylindrical symmetry have x-axis reflection (C_{1h}) symmetry, while particles with z-axis axial or reflection symmetry will in general show no particular symmetry with respect to the x axis.

From Tables V and VI, one can see that the E1+E1 $\rightarrow$E1 channel is available for SHG in all noncentrosymmetric particles with linearly polarized FW plane-wave illumination.[17] In particular, if the particle exhibits C_2 symmetry either around the z or the x axis, SH emission will be given by an oscillating dipole parallel to the C_2 symmetry axis.

Using linearly polarized plane-wave illumination, the lowest-order allowed SH emission channels for centrosymmetric particles with cylindrical symmetry around z (and thus C_{1h} symmetry around x) are E1+E1 $\rightarrow$E2 ($N'_\omega=0$, $N''_\omega=0$, $N_{2\omega}=0$), E1+M1 $\rightarrow$E1 ($M'_\omega=\pm1$, $M''_\omega=\mp1$, $M_{2\omega}=0$), and E1+E2 $\rightarrow$E1 ($M'_\omega=\pm1$, $M''_\omega=\mp1$, $M_{2\omega}=0$).[10,11] Note that electric dipole SH emission is always given by a dipole parallel to z, while the quadrupole SH emission pattern is symmetric around x (see Fig. 3). M1 emission is forbidden[10,11] because the selection rules would lead to $M_{2\omega}=N_{2\omega}=0$, which is a condition that cannot be met since $Y_{10,z}$ and $Y_{10,x}$ are orthogonal to each other.

B. Illumination with a laterally limited light beam

If a coherent converging light beam produced by a high-numerical-aperture objective or even near-field illumination is used to excite the particle, other emission channels become available under the condition that the beam lateral extension is comparable with the particle size. In this case, the beam cannot be considered as a plane wave any longer. Consequences are that a sizable longitudinal component is present and that the rapid spatial variations of the field intensity can increase the relative weight of the higher-order multipoles with respect to a plane wave. This second effect can be easily understood for a converging beam focused by an objective, in which the spot size is limited by diffraction to about $1/k$. If this value is comparable with the particle size a, then the long-wavelength approximation is not valid and higher order multipoles cannot be neglected.

The case of FW illumination through an aperture is more subtle and deserves further discussion. The electromagnetic field in the proximity of a circular aperture at the apex of a metal-coated conical near-field probe can be viewed, to first approximation, as the static-like field produced by an electric and a magnetic dipole oscillating at the fundamental frequency in the center of the aperture.[18] These electric and magnetic dipoles are perpendicular to each other and to the optical axis.[19] In this case, the particle-field interaction Hamiltonian $\hat{\mathbf{p}}\cdot\mathbf{A}$ can be approximated to lowest order by considering only the static interaction between the field sources and the electric dipole, magnetic dipole, and electric quadrupole induced on the particle.

The interaction Hamiltonian $\mathcal{H}'$ between the particle and the staticlike FW field can be approximated as follows:[14]

$$\mathcal{H}' = -\hat{\mathbf{q}}\cdot\mathbf{E}(0) - \hat{\mathbf{m}}\cdot\mathbf{B}(0) - \frac{1}{6}\sum_{i,j=x,y,z}\hat{Q}_{i,j}\frac{\partial E_i}{\partial r_j}(0), \qquad (6)$$

where $\mathbf{E}(0)$ and $\mathbf{B}(0)$ are the electric and magnetic staticlike fields at the particle position, and $\hat{\mathbf{q}}$, $\hat{\mathbf{m}}$, and $\hat{Q}_{i,j}$ are the particle electric dipole, magnetic dipole, and electric quadrupole operators. The three terms in Eq. (6) give origin to the E1, B1, and E2 absorptions of a FW photon, respectively.

The electric quadrupole contribution to the interaction Hamiltonian in Eq. (6) is proportional to the space derivatives $\partial E_i/\partial r_j$ of the electric field at the particle position. In the proximity of the aperture, these do not depend just on the FW far-field wavelength k as in a nonconfined propagating wave. In this region, the electric field is characterized by a superposition of waves with high imaginary-part wave vectors.[4] Their magnitude is of the order of $1/d$, d being the near-field aperture diameter.[4] Therefore, the ratio between the E1 and E2 FW absorption matrix elements does not scale as $(ka)^{-1}$ but rather as d/a, which might be of the order of unity. For this reason, even when the E1+E1→E1 channel is allowed, the latter might not be the only relevant one. Other relevant channels might be E1+E2→E1 or even E2+E2→E1, while M1 or E2 emission can be reasonably ruled out (unless they represent the only allowed channels) sincethe contributions of the E2 and M1 multiplets to the average irradiated power will still be weaker by a factor of the order of $(ka)^{-2}$ with respect to E1 emission.

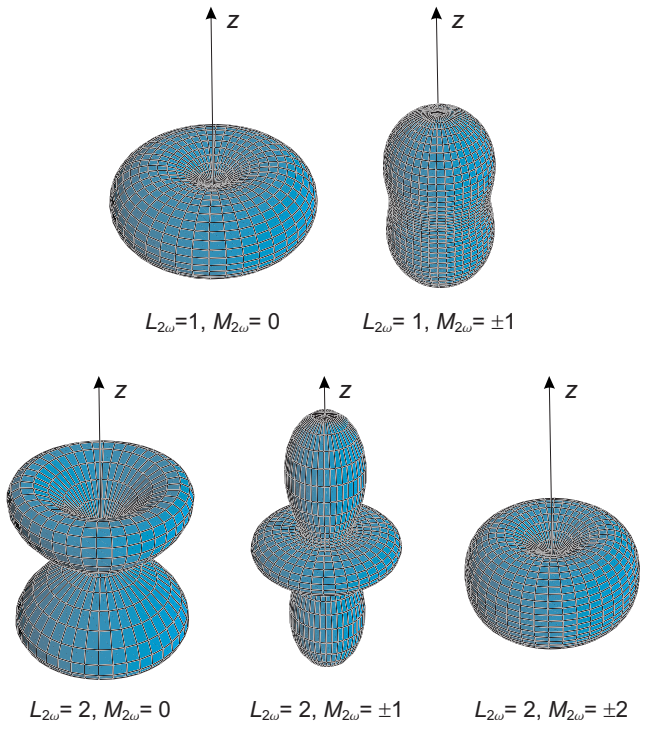

FIG. 3. (Color online) Graphical representation of emission patterns $\frac{dP}{d\Omega}(L_{2\omega},M_{2\omega})$ for dipoles (upper row) and quadrupoles (lower row). The time-averaged radiated power per unit solid angle displays cylindrical symmetry around the quantization axis z.

In calculating the allowed SHG transitions, both for near-field and focused beam FW illumination, one must consider that the particle is not necessarily located on the optical axis. For instance, a subwavelength aperture is raster scanned over the particle in scanning near field microscopy. Under these conditions, the particle will sense a FW electric (magnetic) field with a longitudinal component and, in the case of linearly polarized light coupled to the objective or to the aperture, with a transverse component perpendicular to the impinging electric (magnetic) field.[4] The consequence is that photons with L_z quantum number $M_\omega=0$ can also be absorbed by the particle from a linearly polarized FW field, a possibility excluded by plane-wave illumination. For the same reason, FW photons with $M_\omega=0,\pm1,\pm2$ are available for E2 absorption. Therefore, SH emission channels that would generally be forbidden under far-field FW plane-wave illumination might thus become allowed under FW near-field or converging beam illumination. For example, SHG given by an electric dipole oriented *parallel* to FW electric field linear polarization can be obtained even in a spherical particle,[20] as indicated, for instance, by the fact that the 3-j

TABLE III. Selection rules for E1+E1→E1 second-harmonic emission in particles with axial (C_2) symmetry with respect to z.

Incoming photons L_z quantum numbers		Allowed second harmonic emission
M'_ω	M''_ω	$M_{2\omega}$
0	0	0
0	±1	±1
±1	±1	0

symbol associated to $(L'_\omega=1, M'_\omega=0)$, $(L''_\omega=2, M''_\omega=\pm 1)$, and $(L_{2\omega}=1, M_{2\omega}=\mp 1)$ is nonzero. The corresponding T terms would represent SHG induced by combined electric dipole and quadrupole FW photon absorption from *perpendicular*field components,[21] which is not possible for plane-wave illumination.

As a highly relevant application, let us consider lithographed particles on a substrate (see Fig. 4), such as those employed in surface-enhanced spectroscopy techniques. It is common practice to locally characterize these samples by scanning far-field or near-field microscopy. The presence of the substrate breaks the inversion symmetry with respect to the particle center. For ellipsoidal-shaped dots as those described in Refs. 6 and 22, the particle symmetry group reduces to C_{2v}. In this case, the selection rules governing SHG in C_2 symmetry around the z axis must apply, z being the substrate normal, which is taken parallel to the optical axis. When such particles are excited with a FW plane wave with $\mathbf{k}\|z$ and considering only the lowest-order E1 transitions, M'_ω and M''_ω can only assume the values ±1 both for linearly and circularly polarized light, so parity is conserved only for $M_{2\omega}=0$, corresponding to SH emission from an electric dipole parallel to $\mathbf{k}$ and z [see Fig. 4(a)], as demonstrated in the previous section. The particles also belong to the C_{1h} symmetry group defined with respect to either the x or y axis, oriented parallel to the in-plane principal axes of the ellipsoids. However, this further symmetry does not provide more restrictive selection rules.

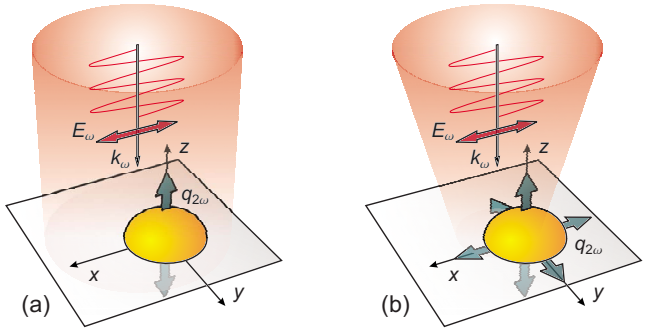

FIG. 4. (Color online) Allowed E1 second-harmonic emission channels for a particle with C_2 symmetry (axial particle over a substrate) excited by (a) a plane wave or (b) a laterally limited beam. The allowed directions of the particle electric dipole $q_{2\omega}$ generating the E1 second-harmonic radiation are indicated by the double-headed arrows on the particle.

When the particles are excited using a focused FW beam or the near field of an aperture, photons with $M_\omega=0$ can be absorbed even from a linearly polarized excitation beam, which means that new channels are open. Considering E1+E1→E1 excitations, the L_z quantum number of the incoming photons can assume all the values $M_\omega=0,\pm 1$. A complete set of selection rules for converging illumination and particles with axial symmetry around z is given in Table III. It basically shows that all channels with E1 emission are now available for the SHG process [see Fig. 4(b)]. The dominant one will be determined by the particle fine structure, which defines the relative strength of each channel.

V. SUMMARY AND CONCLUSIONS

In conclusion, SHG selection rules for nanoparticles have been derived from general conservation laws for photon parity and angular momentum. A complete set of rules has been given for different particle geometries, different polarizations, and different multipole contributions to the matrix elements describing the particle interactions with FW and SH fields. We show that peculiar emission channels that are allowed only when using nonuniform converging illumination can be addressed. Some general interest examples, such as spherical particles in an isotropic environment and ellipsoidal particles on a substrate, have been discussed with some more detail.

ACKNOWLEDGMENTS

The authors would like to acknowledge G. Cerullo and M. Zavelani-Rossi for helpful discussion.

APPENDIX: SELECTION RULES FOR PLANE-WAVE ILLUMINATION

We provide a set of tables (Tables IV–VI) listing the allowed and forbidden SH emission channels for FW plane-wave illumination with different light polarizations and particle symmetries.

TABLE IV. SHG selection rules for the different particle symmetries illustrated in Fig. 2, under circularly polarized far-field plane-wave illumination. Every transition multipole is considered separately. The propagation direction (z axis) is chosen as the quantization axis.

Symmetry and point group	$E_1+E_1\rightarrow E_1$	$E_1+E_1\rightarrow E_2$	$E_1+E_2\rightarrow E_1$	$E_1+M_1\rightarrow E_1$	$E_1+E_1\rightarrow M_1$
Spherical	Forbidden	Allowed for $M_{2\omega}=+2$ or -2	Forbidden	Forbidden	Forbidden
Cylindrical	Forbidden	Allowed for $M_{2\omega}=+2$ or -2	Forbidden	Forbidden	Forbidden
Central, S_2	Forbidden	Allowed	Allowed	Allowed	Allowed
Axial, C_2	Allowed for $M_{2\omega}=0$	Allowed for $M_{2\omega}=0,\pm 2$	Allowed for $M_{2\omega}=0$	Allowed for $M_{2\omega}=0$	Allowed for $M_{2\omega}=0$
Reflection, C_{1h}	Allowed for $M_{2\omega}=\pm 1$	Allowed for $M_{2\omega}=0,\pm 2$	Allowed for $M_{2\omega}=0$	Allowed for $M_{2\omega}=0$	Allowed for $M_{2\omega}=0$

TABLE V. SHG selection rules for the different particle symmetries illustrated in Fig. 2, under linearly polarized far-field plane-wave illumination. The propagation direction (z axis) is chosen as the quantization axis.

Symmetry and point group	$E_1+E_1\rightarrow E_1$	$E_1+E_1\rightarrow E_2$	$E_1+E_2\rightarrow E_1$	$E_1+M_1\rightarrow E_1$	$E_1+E_1\rightarrow M_1$
Spherical	Forbidden	Allowed for $M_{2\omega}=0,\pm 2$	Allowed for $M_{2\omega}=0$	Allowed for $M_{2\omega}=0$	Forbidden
Cylindrical	Allowed for $M_{2\omega}=0$	Allowed for $M_{2\omega}=0,\pm 2$	Allowed for $M_{2\omega}=0$	Allowed for $M_{2\omega}=0$	Forbidden
Central, S_2	Forbidden	Allowed	Allowed	Allowed	Allowed
Axial, C_2	Allowed for $M_{2\omega}=0$	Allowed for $M_{2\omega}=0,\pm 2$	Allowed for $M_{2\omega}=0$	Allowed for $M_{2\omega}=0$	Allowed for $M_{2\omega}=0$
Reflection, C_{1h}	Allowed for $M_{2\omega}=\pm 1$	Allowed for $M_{2\omega}=0,\pm 2$	Allowed for $M_{2\omega}=0$	Allowed for $M_{2\omega}=0$	Allowed for $M_{2\omega}=0$

TABLE VI. SHG selection rules for the different particle symmetries illustrated in Fig. 2, under linearly polarized far-field plane-wave illumination. The electric-field polarization direction (x axis) is chosen as the quantization axis.

Symmetry and point group	$E_1+E_1\rightarrow E_1$	$E_1+E_1\rightarrow E_2$	$E_1+E_2\rightarrow E_1$	$E_1+M_1\rightarrow E_1$	$E_1+E_1\rightarrow M_1$
Spherical	Forbidden	Allowed for $N_{2\omega}=0$	Allowed for $N_{2\omega}=\pm 1$	Allowed for $N_{2\omega}=\pm 1$	Forbidden
Cylindrical	Allowed for $N_{2\omega}=0$	Allowed for $N_{2\omega}=0,\pm 2$	Allowed for $N_{2\omega}=\pm 1$	Allowed for $N_{2\omega}=\pm 1$	Allowed for $N_{2\omega}=0$
Central, S_2	Forbidden	Allowed	Allowed	Allowed	Allowed
Axial, C_2	Allowed for $N_{2\omega}=0$	Allowed for $N_{2\omega}=0,\pm 2$	Allowed for $N_{2\omega}=\pm 1$	Allowed for $N_{2\omega}=\pm 1$	Allowed for $N_{2\omega}=0$
Reflection, C_{1h}	Allowed for $N_{2\omega}=\pm 1$	Allowed for $N_{2\omega}=0,\pm 2$	Allowed for $N_{2\omega}=\pm 1$	Allowed for $N_{2\omega}=\pm 1$	Allowed for $N_{2\omega}=0$

*marco.finazzi@fisi.polimi.it

[1] P. A. Franken, A. E. Hill, C. W. Peters, and G. Weinreich, Phys. Rev. Lett. **7**, 118 (1961).
[2] N. Bloembergen and P. S. Pershan, Phys. Rev. **128**, 606 (1962).
[3] For reviews, see, e.g., Y. R. Shen, Annu. Rev. Phys. Chem. **40**, 327 (1989); J. F. Mc Gilp, J. Phys. D **29**, 1812 (1996); N. Bloembergen, Appl. Phys. B: Lasers Opt. **68**, 289 (1999); G. Lüpke, Surf. Sci. Rep. **35**, 75 (1999); M. C. Downer, B. S. Mendoza, and V. I. Gavrilenko, Surf. Interface Anal. **31**, 966 (2001).
[4] L. Novotny and B. Hecht, *Principles of Nano-Optics* (Cambridge University Press, Cambridge, 2006).
[5] S. Nie and S. R. Emory, Science **275**, 1102 (1997).
[6] J. Grand, S. Kostcheev, J.-L. Bijeon, M. Lamy de la Chapelle, P.-M. Adam, A. Rumyantseva, G. Lerondel, and P. Royer, Synth. Met. **139**, 621 (2003).
[7] C. M. Pitsillides, E. K. Joe, X. Wei, R. R. Anderson, and C. P. Lin, Biophys. J. **84**, 4023 (2003).
[8] I. H. El-Sayed, X. Huang, and M. A. El-Sayed, Cancer Lett. **239**, 129 (2006).
[9] S. I. Bozhevolnyi and V. Z. Lozovski, Phys. Rev. B **61**, 11139 (2000); **65**, 235420 (2002).
[10] J. I. Dadap, J. Shan, K. B. Eisenthal, and T. F. Heinz, Phys. Rev. Lett. **83**, 4045 (1999).
[11] J. I. Dadap, J. Shan, and T. F. Heinz, J. Opt. Soc. Am. B **21**, 1328 (2004).
[12] V. L. Brudny, B. S. Mendoza, and W. L. Mochán, Phys. Rev. B **62**, 11152 (2000).
[13] W. L. Mochán, J. A. Maytorena, B. S. Mendoza, and V. L. Brudny, Phys. Rev. B **68**, 085318 (2003).
[14] J. D. Jackson, *Classical Electrodynamics* (Wiley, New York, 1975).
[15] D. M. Brink and G. R. Satchler, *Angular Momentum* (Oxford University Press, London, 1993).
[16] M. Tinkham, *Group Theory and Quantum Mechanics* (McGraw-Hill, New York, 1964).
[17] J. Nappa, I. Russier-Antoine, E. Benichou, Ch. Jonin, and P. F. Brevet, J. Chem. Phys. **125**, 184712 (2006).
[18] A. Drezet, M. J. Nasse, S. Huant, and J. C. Woehl, Europhys. Lett. **66**, 41 (2004).
[19] At variance with the classic Bethe-Bouwkamp model for a subwavelength hole in a perfectly conducting screen [C. J. Bouwkamp, Philips Res. Rep. **5**, 321 (1950)], which introduces an electric dipole perpendicular to the screen, we consider an electric dipole in the plane of the aperture, which has been shown to be a better description for a real near-field probe (Ref. 18).
[20] J. Nappa, G. Revillod, I. Russier-Antoine, E. Benichou, C. Jonin, and P. F. Brevet, Phys. Rev. B **71**, 165407 (2005).
[21] P. Figliozzi, L. Sun, Y. Jiang, N. Matlis, B. Mattern, M. C. Downer, S. P. Withrow, C. W. White, W. L. Mochán, and B. S. Mendoza, Phys. Rev. Lett. **94**, 047401 (2005).
[22] M. Celebrano, M. Zavelani-Rossi, D. Polli, G. Cerullo, P. Biagioni, M. Finazzi, L. Duò, M. Labardi, M. Allegrini, J. Grand, and P.-M. Adam, J. Microsc. (to be published).